

Pauli blocking versus electrostatic attenuation of optical transition intensities in charged PbSe quantum dots

J. M. An, A. Franceschetti, and Alex Zunger

National Renewable Energy Laboratory, Golden, Colorado 80401, USA

(Received 29 August 2007; published 26 October 2007)

Quantum dots can be charged selectively by electrons or holes. This leads to changes in the intensity of interband and intraband optical transitions. Using atomistic pseudopotential calculations, we show that (i) when carriers are injected into *dot-interior* quantum-confined states, the intensity of interband transitions that have those states as their initial or final states is attenuated (“Pauli blocking”) and (ii) when carriers are injected into *localized* states near the surface of the dots, the electrostatic field set up by these charges attenuates all optically allowed interband transitions. We describe and explain these two mechanisms of intensity attenuation in the case of charged PbSe quantum dots. In addition, this study reveals a new assignment of the peaks in the absorption spectrum. The absorption spectrum of charged PbSe dots was previously interpreted assuming that all injected electrons reside in dot-interior states. This assumption has led to the suggestion that the second absorption peak originates from S_h-P_e and P_h-S_e optical transitions, despite the fact that such transitions are expected to be dipole forbidden. Our results show that the observed bleaching of absorption peaks upon electron or hole charging does not imply that the S_h-P_e or P_h-S_e transitions are allowed. Instead, the observed bleaching sequence is consistent with charging of both dot-interior and surface-localized states and with the assignment of the second absorption peak to the allowed P_h-P_e transition.

DOI: [10.1103/PhysRevB.76.161310](https://doi.org/10.1103/PhysRevB.76.161310)

PACS number(s): 73.21.La, 71.15.-m, 78.20.-e

One of the interesting aspects of quantum-dot physics is the ability to load a significant number of electrons or holes into them, and measure for each charge state the change in free energy (“charging energy”) and the change in the optical excitation spectrum.¹⁻⁸ Charging has been accomplished in colloidal dots via injection of carriers from an STM tip¹⁻³ or via electrochemical methods,⁴ and in self-assembled epitaxial dots via metallic gates.⁵⁻⁸ Such experiments, and corresponding theories,^{9,10} have demonstrated a nontrivial dependence of the addition energies on the number of added carriers, including the emergence of “Coulomb blockade”⁵⁻⁷ and the violation of Hund’s rule⁹ and the Aufbau principle.^{8,9} Less explored are the effects of dot charging on the intensity of the optical transitions. Such effects are important because many applications of quantum dots rely on absorption or emission of light. Here one can anticipate interesting effects, depending on the nature of the states occupied by the added charges:

(i) *Attenuation of the intensity of the lowest-energy interband absorption peak.* Such attenuation can occur due to filling of the band-edge states by electrons or holes (“Pauli blocking”). This effect is analogous to the “Moss-Burstein” shift¹¹ in doped semiconductors, where occupation of the conduction band by carriers attenuates the corresponding interband transitions. Trapping of carriers near the surface of the dot can also attenuate the first interband absorption peak, because the electrostatic field set up by the trapped charge(s) tends to spatially separate the photogenerated electron-hole pair.

(ii) *Attenuation of the intensity of higher-energy interband absorption peaks.* If the injected carriers occupy dot-interior states, only interband transitions that have those states as initial or final states will be attenuated by Pauli blocking. Thus Pauli blocking of high-energy interband transitions requires loading multiple carriers into the dot. On the other

hand, if the injected carriers occupy states localized near the surface of the dot, the intensity of *every absorption peak* will be attenuated by electrostatic effects. Thus a few carriers trapped near the surface will cause electrostatic attenuation of high-energy interband transitions.

(iii) *Shift of interband transition energies due to charging.* An electron loaded into a quantum dot creates an electrostatic field that repels the photogenerated electron and attracts the photogenerated hole. If the electron is injected into a dot-interior state (e.g., $e1$), the fundamental $e0-h0$ exciton energy will shift by $J_{e1,e0} - J_{e1,h0}$. Depending on the relative degree of localization of the electron and the hole wave functions, this could result in either a redshift or a blueshift of the fundamental exciton. If the electron is injected in a localized state near the surface, the resulting electrostatic field will lead to a Stark shift of interband transitions.

(iv) *Symmetry lowering of orbitals due to surface charging.* If the loaded charge is sufficiently localized, its associated electric field could deform the orbitals so as to render otherwise forbidden transitions (e.g., S -to- P or P -to- S) allowed.

(v) *Blinking of photoluminescence intensity.* In addition to changes in the absorption spectrum, charging may lead to blinking and spectral diffusion of the emission spectrum. These effects have been reported for many semiconductor nanocrystals, and have been attributed to the presence of charges either in the interior of the nanocrystal,¹² or at the surface of the nanocrystals.¹³

Effects (i)–(v) are general phenomena that occur in all colloidal quantum dots. Pauli blocking and electrostatic attenuation of optical transitions are detrimental to any application of quantum dots in optical devices requiring light absorption, such as quantum-dot-based solar cells,^{14,15} because they tend to reduce the absorption coefficient of the dots. Thus, a fundamental understanding of the effects of charging

on the intensity of interband transitions, and a quantitative determination of the relative importance of Pauli blocking and electrostatic attenuation have important implications for the development of nanoscale optical devices. In this work we use atomistic pseudopotential calculations to investigate the effects of charging on interband optical transitions in PbSe colloidal quantum dots. PbSe quantum dots happen to be experimentally very well studied in this respect. Moreover, unlike the case of CdSe quantum dots,¹⁶ the physical origin of the absorption peaks of PbSe quantum dots is still controversial. Indeed, the second absorption peak has been attributed by several authors^{4,17-21} to the S_h - P_e and P_h - S_e interband cross transitions, despite the fact that such transitions are parity forbidden, and therefore should have negligible oscillator strength. This assignment was supported by recent experimental measurements of the absorption spectrum of *charged* PbSe quantum dots,⁴ although none of the existing studies has been able to clarify the mechanism by which an optically forbidden transition becomes allowed. Our results show that the observed bleaching of absorption peaks upon electron-hole charging⁴ does not imply that S_h - P_e or P_h - S_e transitions are allowed in PbSe quantum dots. Instead, the observed bleaching sequence is consistent with charging of both dot-interior and surface-localized states and with the assignment of the second absorption peak to the allowed P_h - P_e transition.

The band-edge states of PbSe dots are fourfold degenerate (eightfold degenerate including spin), because they derive from the four degenerate L valleys of the fcc bulk Brillouin zone.²² Above this set of eight S -like states lies a set of 24 P -like states. Since the bulk L valleys have anisotropic effective masses, the P -like states split into a group of eight states derived from the parallel component of the L valley (P^{\parallel}), and a group of 16 states derived primarily from the perpendicular component of the L valley (P^{\perp}). In the absorption spectrum of a *neutral* PbSe quantum dot,²³ the first allowed interband transition (α) occurs between S_h and S_e , and has 64 fine-structure components, on account of the eightfold degeneracy of both S_h and S_e . The second allowed transition (β) is P_h^{\parallel} - P_e^{\parallel} , while the third allowed transition (δ) is P_h^{\perp} - P_e^{\perp} . The P_h^{\parallel} - P_e^{\perp} transition (γ), located above β , is only weakly allowed, while the S_h - P_e and P_h - S_e cross transitions are orbitally forbidden, and do not carry oscillator strength.

Our study of the effects of charging on the interband optical transitions shows that (i) carriers injected into dot-interior S -like states attenuate the first (S_h - S_e) absorption peak (Pauli blocking), but do not attenuate the second (P_h^{\parallel} - P_e^{\parallel}) absorption peak. However, (ii) if the injected charge is localized near the dot surface, the resulting electrostatic field attenuates both the first and the second absorption peaks, in agreement with the experimental results of Wehrenberg and Guyot-Sionnest.⁴ (iii) Loading electrons into the dot interior shifts the S_h - S_e transition by a few meV, while the redshift due to surface charging (Stark shift) is ~ 10 meV. (iv) Surface charging renders the S - P and P - S interband transitions weakly allowed, because of field-induced orbital distortions. These transitions occur at slightly lower energies than the P_h - P_e transition.

Method. We use the following two steps to calculate the

optical absorption spectra of charged quantum dots.

In step 1, we solve for the single-particle energy eigenstates of a quantum dot using the effective Schrödinger equation:

$$\left[-\frac{1}{2}\nabla^2 + V_{\text{loc}}(\mathbf{r}) + V_{\text{so}} + V_{\text{ext}}(\mathbf{r}) \right] \psi_i(\mathbf{r}) = \varepsilon_i \psi_i(\mathbf{r}), \quad (1)$$

where the single-particle wave functions $\psi_i(\mathbf{r})$ are expanded in a plane wave basis set, $V_{\text{loc}}(\mathbf{r})$ is the local pseudopotential, V_{so} is the spin-orbit operator, and $V_{\text{ext}}(\mathbf{r})$ is the electrostatic potential generated by an external charge distribution. The local potential, $V_{\text{loc}}(\mathbf{r})$, is represented as a superposition of screened atomic pseudopotentials for atom species α at sites $\mathbf{R}_{n,\alpha}$

$$V_{\text{loc}}(\mathbf{r}) = \sum_{n,\alpha} v_{\alpha}(|\mathbf{r} - \mathbf{R}_{n,\alpha}|). \quad (2)$$

The atomic pseudopotentials are fitted to reproduce bulk properties accurately.²³ Whereas dot-interior states are easy to characterize experimentally and theoretically, localized states in the matrix are not universal, and their nature has not been fully clarified. Thus, to study the effects of localized carriers trapped in the matrix surrounding the dots, we consider a pointlike charge distribution located near the surface of the dot. This approximation is appropriate, because the effects of dipole and multipole moments on the dot-interior states that contribute to the absorption spectrum are small. The resulting electrostatic potential $V_{\text{ext}}(\mathbf{r})$ is obtained by solving the generalized Poisson equation

$$\nabla \cdot \epsilon(\mathbf{r}) \nabla V_{\text{ext}}(\mathbf{r}) = 4\pi\rho(\mathbf{r} - \mathbf{r}_i), \quad (3)$$

where $\rho(\mathbf{r} - \mathbf{r}_i) = A e^{-(\mathbf{r} - \mathbf{r}_i)^2/W^2}$ is a normalized Gaussian charge distribution of width W centered at \mathbf{r}_i , and $\epsilon(\mathbf{r})$ is the position-dependent macroscopic dielectric function. First-principles calculations^{24,25} have shown that $\epsilon(\mathbf{r})$ converges rapidly to its bulk value as the interior of the nanostructure is approached. Thus we use the dielectric function profile $1/\epsilon(\mathbf{r}) = 1/\epsilon_{\text{out}} + [1/\epsilon_{\text{in}} - 1/\epsilon_{\text{out}}]m(\mathbf{r})$, where $\epsilon_{\text{in}} = 22.9$ is the bulk PbSe macroscopic dielectric constant, and $\epsilon_{\text{out}} = 1$ (vacuum). The mask function $m(\mathbf{r})$ decays sinusoidally from 1 to 0 in a ~ 2 Å thick transition region near the dot surface, to mimic the gradual variation of the dielectric constant at the surface of the dot.^{24,25} Equation (3) includes surface-polarization effects via the position-dependent dielectric function $\epsilon(\mathbf{r})$. The electrostatic potential $V_{\text{ext}}(\mathbf{r})$ obtained from the Poisson equation [Eq. (3)] is then used in the solution of the Schrödinger equation [Eq. (1)].

In step 2, we calculate the electron-hole Coulomb and exchange integrals using the single-particle wave functions $\psi_i(\mathbf{r})$ of Eq. (1). The excited-state energies $E_{\gamma}(N_h, N_e)$ and wave functions $\Psi_{\gamma}(N_h, N_e)$ of a quantum dot containing N_e electrons and N_h holes are obtained by diagonalizing the configuration-interaction (CI) Hamiltonian in a basis set of Slater determinants obtained by placing N_e electrons in the conduction band and N_h holes in the valence band.²⁶ The CI basis set was constructed using 40 valence states and 16 conduction states. The dipole matrix elements between many-particle states are given by

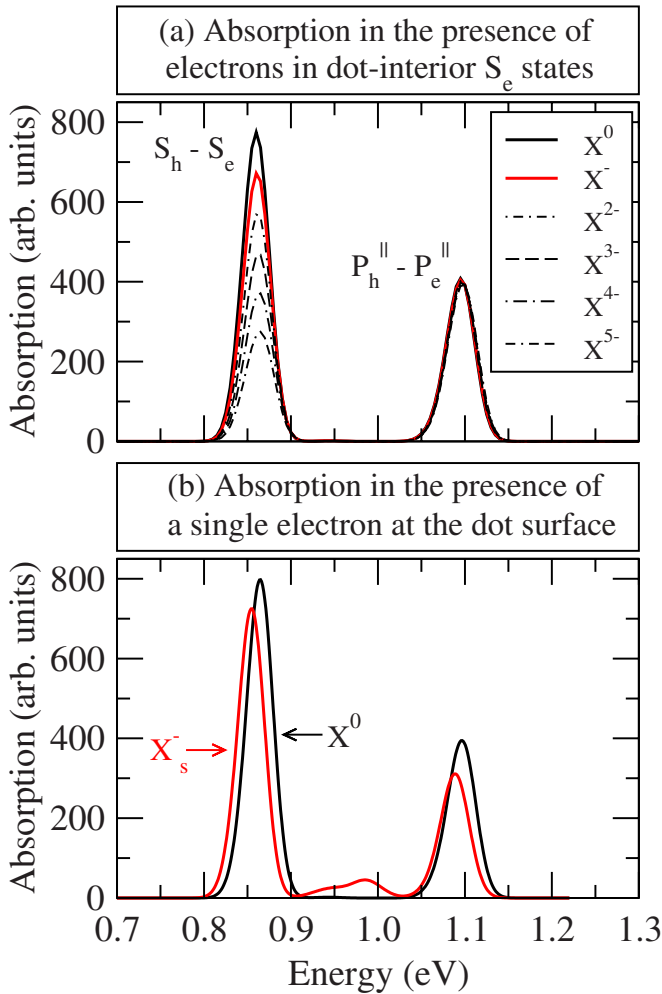


FIG. 1. (Color online) Calculated optical absorption spectra of a 30.6 Å PbSe quantum dot. (a) Absorption spectrum of the neutral exciton (X^0), and the negatively charged excitons (X^- – X^{5-}). (b) Absorption spectrum in the presence of a negative point charge localized near the dot surface. The transitions were broadened using a 20 meV wide Gaussian convolution function, to account for inhomogeneous broadening due to size-distribution effects.

$$\mathbf{M}_\gamma = \langle \Psi_0(N_h, N_e) | \mathbf{r} | \Psi_\gamma(N_h + 1, N_e + 1) \rangle, \quad (4)$$

where $\Psi_0(N_h, N_e)$ is the ground-state, many-particle wave function of the dot with $N_h + N_e$ spectator carriers. Finally, the absorption spectrum is calculated as

$$I(\omega) \sim \sum_\gamma |\mathbf{M}_\gamma|^2 \delta(\hbar\omega - E_\gamma + E_0). \quad (5)$$

We consider here a PbSe quantum dot of radius $R = 30.6$ Å (Pb₂₀₄₆Se₂₁₁₇). The dot has the rocksalt lattice structure (lattice constant $a = 6.117$ Å), and is constructed by placing a Se atom at the center of a sphere with an effective radius R and then adding Pb and Se atoms within R according to the rocksalt structure. For such large dots, the electronic properties do not change much if we place a Pb atom at the dot center. The dangling bonds at the surface of the quantum dot are passivated by “ligand potentials,” in order to remove all surface states from the dot band gap to ~ 1 eV

away from the band edges. Reference 23 depicts our calculated interband spectra as well as intraband excitations using this approach.

Results. Figure 1(a) shows the calculated optical absorption spectrum in the presence of N_e spectator electrons occupying the dot-interior S_e levels. When spectator electrons occupy dot-interior states, wave-function rearrangements induced by the spectator charges are small, so the CI Hamiltonian was solved in the single-configuration approximation. Figure 1(b) shows the calculated full-CI absorption spectra in the presence of a single negative pointlike charge trapped near the surface of the quantum dot. Referring to the questions raised in (i)–(iv) above, we find the following.

(a) *Effects of occupying dot-interior, quantum-confined levels by spectator electrons.* We see from Fig. 1(a) that (i) the intensity of the first interband transition (S_h – S_e) is attenuated by a factor $\sim 1/8$ for each electron injected into the S_e states, as expected from Pauli blocking. The intensity attenuation scales approximately linearly with the number of loaded electrons. (ii) The intensity of the second interband transition ($P_h^||$ – $P_e^||$) is unaffected by charging the S_e levels. (iii) There is no oscillator strength in the intermediate energy between S_h – S_e and $P_h^||$ – $P_e^||$, as expected from the forbidden nature of the S_h – P_e and P_h – S_e cross transitions. (iv) The spectral shift upon charging is negligible, in agreement with Schaller *et al.*²⁷ Note that the intensity of the $P_h^||$ – $P_e^||$ absorption peak is lower than that of the S_h – S_e peak, because of the smaller oscillator strength of P – P transitions and the fact that many of the fine-structure transitions under $P_h^||$ – $P_e^||$ are dark due to electron-hole exchange interactions.²⁸

(b) *Effects of occupying localized states near the surface of the dot.* Figure 1(b) shows the calculated optical absorption spectrum of a $R = 30.6$ Å PbSe dot, where a negative pointlike charge has been placed near its surface. We see that (i) the intensity of both the first (S_h – S_e) and the second ($P_h^||$ – $P_e^||$) absorption peaks are attenuated in response to charging. Thus, whereas charging of dot-interior S_e quantum states [Fig. 1(a)] can Pauli-block only interband transitions that have S_e as their final states (i.e., S_h – S_e but not P_h – P_e), charging of localized states near the surface of the dots [Fig. 1(b)] can attenuate all interband transitions, including the $P_h^||$ – $P_e^||$ transition. The degree of bleaching of a given absorption peak can be computed by taking the area of the peak with (A_s) and without (A_0) spectator electrons. We find that $A_s/A_0 \approx 0.91$ for the first absorption peak, and $A_s/A_0 \approx 0.79$ for the second absorption peak. (ii) In the presence of a charge localized near the surface of the dot, there is an intensity buildup in the energy range between the S_h – S_e and the $P_h^||$ – $P_e^||$ absorption peaks. Analysis of the eigenvalues contributing to transitions in this energy window shows that this intensity build-up is associated with the S_h – P_e and P_h – S_e interband transitions, located around 0.9–1.0 eV. Indeed, we find that transitions that are *dipole-forbidden* in a neutral dot (e.g., S_h – P_e or P_h – S_e) are *enhanced* when surface charges are present. The reason is that the electrostatic field set up by localized surface charges causes the S and P envelope functions to have finite, nonzero overlap. (iii) In the presence of a localized surface charge, the absorption peaks are redshifted relative to the neutral dot. The calculated redshift is

10 meV for the S_h - S_e absorption peak and 7 meV for P_h^{\parallel} - P_e^{\parallel} . This redshift is due to the electrostatic field induced by the surface charge. Effects (i)–(iii) discussed above decrease in magnitude as the distance of the charge from the surface of the dot increases. However, due to the long-range nature of the Coulomb interaction, these effects will still be present even if the charge is localized at a distance of several Å from the surface of the dot.

Previously, numerous authors^{4,17–21} have interpreted the first and second absorption peaks as originating from the S_h - S_e and P_h - S_e (or S_h - P_e) transitions, respectively. This was initially based on the coincidence of the measured position of the second peak with the calculated P_h - S_e and S_h - P_e transition energies in a $k \cdot p$ model calculation.¹⁷ However, more accurate, atomistic pseudopotential calculations²³ have shown that the energy of the second measured absorption peak agrees with the calculated P_h^{\parallel} - P_e^{\parallel} transition. Indeed, we found²³ that the S_h - P_e and P_h - S_e transitions have extremely low intensity in a neutral PbSe dot, and one cannot attribute the observed second absorption peak to those transitions. Thus, we have interpreted²³ the first and second absorption peaks as being S_h - S_e and P_h^{\parallel} - P_e^{\parallel} , respectively. This assignment agrees very well with recent tunneling spectroscopy measurements.¹ In those experiments the authors first measured, via single electron tunnelling, the energy differences between the P_h and P_e levels, and between the S_h and P_e levels. Then, by comparing these energy differences with the peaks in the absorption spectra, they were able to ascertain that the second absorption peak corresponds to the P_h - P_e energy difference obtained from tunneling, whereas the S_h - P_e energy difference obtained from tunneling fell short by a few hundreds meV from the energy of the second absorption peak.

Wehrenberg and Guyot-Sionnest⁴ observed a concurrent reduction in the intensity of the first and second interband absorption peaks in PbSe quantum dots as electrons or holes were loaded into the dots. They concluded that the second absorption peak must involve S_e final states, which are directly populated by the injected electrons. However, as noted above, the intensity reduction of the second absorption peak upon electron charging does not necessarily imply that this peak originates from interband transitions into the S_e states. For example, if some of the injected charges occupy the S_e states and others are trapped in localized states near the surface of the dots, one would observe attenuation of both the S_h - S_e transition and the P_h^{\parallel} - P_e^{\parallel} transition, as the effects of interior charging and surface charging would add up. Indeed, Fig. 1(b) demonstrates that if some fraction of the injected carriers ends up in localized states near the surface of the dots, both the first and second absorption peaks are attenuated, even though the second peak (P_h^{\parallel} - P_e^{\parallel}) has a different final state than the first peak (S_h - S_e). We conclude that the theoretical evidence is fully consistent with the interpretation that the first and second observed peaks correspond to the S_h - S_e and P_h^{\parallel} - P_e^{\parallel} transitions, respectively, and that the S_h - P_e and P_h - S_e cross transitions have vanishing intensity, unless some charge is trapped near the dot surface, breaking the symmetry.

We thank P. Guyot-Sionnest for illuminating discussions on the experiments and interpretation of PbSe dot charging. This work was funded by the U.S. Department of Energy, Office of Science, Basic Energy Science, under Contract No. DE-AC36-99GO10337 to NREL.

- ¹P. Liljeroth, P. A. ZeijlmansvanEmmichoven, S. G. Hickey, H. Weller, B. Grandidier, G. Allan, and D. Vanmaekelbergh, *Phys. Rev. Lett.* **95**, 086801 (2005).
- ²U. Banin, Y. Cao, D. Katz, and O. Millo, *Nature (London)* **400**, 542 (1999).
- ³E. P. A. M. Bakkers *et al.*, *Nano Lett.* **1**, 551 (2001).
- ⁴B. L. Wehrenberg and P. Guyot-Sionnest, *J. Am. Chem. Soc.* **125**, 7807 (2003).
- ⁵M. Kastner, *Phys. Today* **46**, 24 (1993).
- ⁶S. Tarucha, D. G. Austing, T. Honda, R. J. vanderHage, and L. P. Kouwenhoven, *Phys. Rev. Lett.* **77**, 3613 (1996).
- ⁷L. P. Kouwenhoven *et al.*, *Science* **278**, 1788 (1997).
- ⁸M. Ediger, G. Bester, B. D. Gerardot, A. Badolato, P. M. Petroff, K. Karrai, A. Zunger, and R. J. Warburton, *Phys. Rev. Lett.* **98**, 036808 (2007).
- ⁹A. Franceschetti and A. Zunger, *Europhys. Lett.* **50**, 243 (2000).
- ¹⁰L. He, G. Bester, and A. Zunger, *Phys. Rev. Lett.* **95**, 246804 (2005); L. He and A. Zunger, *Phys. Rev. B* **73**, 115324 (2006).
- ¹¹T. S. Moss, *Proc. Phys. Soc. London, Sect. B* **67**, 775 (1954); E. Burstein, *Phys. Rev.* **93**, 632 (1954).
- ¹²M. Nirmal *et al.*, *Nature (London)* **383**, 802 (1996).
- ¹³L. W. Wang, *J. Phys. Chem. B* **109**, 23330 (2005).
- ¹⁴R. D. Schaller and V. I. Klimov, *Phys. Rev. Lett.* **92**, 186601

- (2004).
- ¹⁵A. Luque and A. Marti, *Phys. Rev. Lett.* **78**, 5014 (1997).
- ¹⁶L. W. Wang and A. Zunger, *J. Phys. Chem. B* **102**, 6449 (1998).
- ¹⁷I. Kang and F. W. Wise, *J. Opt. Soc. Am. B* **14**, 1632 (1997).
- ¹⁸R. D. Schaller, J. M. Pietryga, S. V. Goupalov, M. A. Petruska, S. A. Ivanov, and V. I. Klimov, *Phys. Rev. Lett.* **95**, 196401 (2005).
- ¹⁹R. J. Ellingson *et al.*, *Nano Lett.* **5**, 865 (2005).
- ²⁰J. M. Harbold, H. Du, T. D. Krauss, K. S. Cho, C. B. Murray, and F. W. Wise, *Phys. Rev. B* **72**, 195312 (2005).
- ²¹G. Allan and C. Delerue, *Phys. Rev. B* **70**, 245321 (2004).
- ²²S. H. Wei and A. Zunger, *Phys. Rev. B* **55**, 13605 (1997).
- ²³J. M. An, A. Franceschetti, S. V. Dudiy, and A. Zunger, *Nano Lett.* **6**, 2728 (2006).
- ²⁴C. Delerue, M. Lannoo, and G. Allan, *Phys. Rev. B* **68**, 115411 (2003).
- ²⁵X. Cartoixa and L. W. Wang, *Phys. Rev. Lett.* **94**, 236804 (2005).
- ²⁶A. Franceschetti, H. X. Fu, L. W. Wang, and A. Zunger, *Phys. Rev. B* **60**, 1819 (1999).
- ²⁷R. D. Schaller, M. A. Petruska, and V. I. Klimov, *J. Phys. Chem. B* **107**, 13765 (2003).
- ²⁸J. M. An, A. Franceschetti, and A. Zunger, *Nano Lett.* **7**, 2129 (2007).